17th Australasian Fluid Mechanics Conference
Auckland, New Zealand
5-9 December 2010

Shear rate gradients within an *in vitro* thrombotic environment.

C. J. Butler, K. Ryan and G. J. Sheard

Department of Mechanical and Aerospace Engineering,
Monash University, Victoria 3800, Australia

Abstract

The flow of blood past an axisymmetric thrombus analogue, within an *in vitro* geometry, is computed via solution of the three–dimensional (3D) Navier–Stokes equations. A spectral-element / Fourier spatial discretization is used to solve for the flow within the domain. Particle tracking is used to model the Lagrangian behavior of thrombocytes (platelets) throughout the domain and to investigate the temporal gradients of shear rate which occur. Previously we have shown that increasing thrombus size results in significant changes in the maximum shear rate occuring concurrently with topological transitions of shear rate (Butler et al. 2009). This paper shows that despite low Reynolds numbers ($O(1)$) non–linear behavior is observed with respect to shear rate surrounding the thrombus analogue. Investigating the domain with a Lagrangian framework attached to platelets reveals a 'chequerboard' pattern of shear rate gradient. This suggests multiple regions of platelet adhesion may occur. Further studies of shear dependent thrombus growth must investigate both the bulk and local variations in shear rate.

Introduction

Thrombosis, the development of blood clots within the vasculature, presents a significant clinical risk of myocardial infaction, cerebral and pulmonary embolism, and other diseases. Studies have long shown that there is an interaction between vascular diseases and the dynamics of blood flow (for reviews see [11, 4, 20]). However, the investigation of flow effects on thrombus growth is more recent. In general a thrombus is an aggregate of blood cells and proteins bound to a blood vessel wall. The structure of the thrombus under arterial conditions is dominated by platelets. As a result the growth of a thrombus, under arterial conditions, is dependent on the aggregation, adhesion and activation of platelets [6]. An important question may be posed; after initial formation of a thrombus what interactions mediate platelet adhesion and activation after isolation of the injury site?

In addition to the biochemical processes that occur, early studies [2] showed shear force dependent platelet functionality at pathological shear rates ($\gamma \geq 10000$). Further research revealed that shear rate correlates with the adhesive potential of platelets [17, 16]. However, recent research, particularly that of Nesbitt et al. [13], has shown a causal relationship between shear–force and the initial adhesion and recruitment of a platelet to a thrombus. Critically the physical recruitment occurs in the absence of chemical agonists previously thought to be required for recruitment [8]. It was also theorized that spatial 'micro–gradients' of shear are required for shear mediated platelet aggregation [13]. However, earlier research showed platelet functionality varied with temporal shear rate gradient [8]. In this paper we seek to extend our previous work by exploring two effects: The effect of changing bulk flow properties (Reynolds number) on the system, and the behavior of shear rate when considered within Lagrangian, rather than Eulerian, framework.

The current state of the art method for studing platelet adhesion *in vitro* can be found summarized in [12]. Importantly we note that there is no consideration of the non-linear effects of the Navier–Stokes equations on shear rate. Shear rate is approximated globally by Poiseuille flow:

$$\gamma_b = \frac{6\bar{U}}{H}, \tag{1}$$

where $\bar{U}$ is the mean flow velocity, H is the height of the channel and γ_b is the bulk (or wall) shear rate in the two dimensional channel. Our previous work [3] has shown that this simplistic approach is insufficient when considering local gradients surrounding the thrombus. In this paper we seek to show that Reynolds number effects play a significant role in determining shear rate amplitude, despite the low *Re*. Additionally,an appropriate reference frame, in this case a Lagrangian framework attached to the platelets, is important when considering the influence of shear rate variations.

Methodology

The thrombotic geometry considered in this study is a simplified geometry based on the *in vitro* geometry described in [12] such as used by [17, 16, 8, 13] and others. These geometries considered thrombi adhering to the wall of a high aspect ratio (*AR*) micro channel where typically:

$$AR = \frac{W}{H} = 10, \tag{2}$$

where W is the width of the channel and H the height. A thrombus analogue is introduced into the channel, at the centreline, to simulate the thrombus. The thrombus analogue is defined by a partially protruded sphere where the ratio of thrombus height (H_T) to radius (r) is fixed ($0.25 = \frac{H_T}{r}$). The thrombus height within the channel is defined based on the ratio of thrombus height to channel height $h_t = H_T/H$. An example spectral–element mesh is shown in figure 1. The mesh shown is a meridional half plane ($r-z$) which defines the axisymmetric domain over which the flow is solved. The radius of the mesh (L) is such that the mesh reaches the side wall of the channel at the maximum extent. This domain allows an analytical model to be used for the inlet boundary condition which is described in the boundary conditions section.

The Reynolds number for the system is defined as for channel flow:

$$Re = \frac{\bar{U}H}{\nu}, \tag{3}$$

where ν is the kinematic viscosity. Given the high shear rates which *in vitro* experiments typically explore ($\gamma_b \geq 1000$) a Newtonian model for blood flow is valid [15]. Matched to the conditions of [13] a linear relationship between (γ_b) and *Re* is derived as: $Re = 4.34 \times 10^{-3}\gamma_b$. Given this, a parameter space was constructed consisting of a range of biologically relevant shear rates ($1200 \leq \gamma_b \leq 10000$). For each γ_b a range of 21 thrombus heights ($0.02 \leq h_t \leq 0.8$) are considered.

Bulk shear rate (γ_b) as previously defined is sufficient to explore the parameter space when not considering local fluid dynamics.

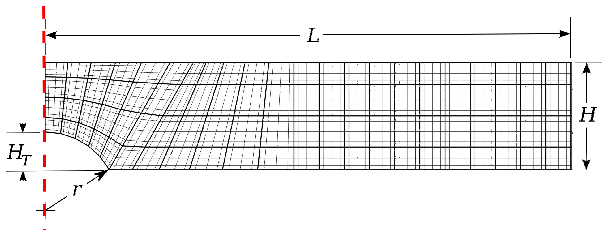

Figure 1: Representative computational mesh diagram, $(r_+ - z)$ plane. Spectral–element boundaries are denoted bold lines. Thin grey lies denote nodal evaluation points. The dashed red line denotes axis of spatial symmetry.

However, shear rate is defined by the rank two strain tensor S as

$$S = \nabla \mathbf{u} + (\nabla \mathbf{u})^{\mathsf{T}}. \tag{4}$$

This definition may be simplified to a scalar shear rate (γ) as:

$$\gamma = \sqrt{2}\sqrt{S:S}. \tag{5}$$

In this study, shear rate is normalized by the bulk upstream conditions,

$$\chi = \frac{\gamma}{\gamma_b}, \tag{6}$$

non–dimensionalizing shear rate in a fashion such that the undisturbed system (without a thrombus) has a maximum of $\chi = 1$.

Numerical Techniques

This study considers blood as an incompressible, Newtonian fluid. The flow is considered to be unsteady within the previously described channel. This approximation yields the Navier–Stokes equations to be solved as

$$\frac{\partial \mathbf{u}}{\partial t} + \mathbf{u}\cdot\nabla\mathbf{u} = -\nabla P + \nu\nabla^2\mathbf{u}, \tag{7}$$

$$\nabla\cdot\mathbf{u} = 0, \tag{8}$$

where ν is the kinematic viscosity, $\mathbf{u}$ is the velocity vector field and P is the kinematic pressure field. The momentum equation is integrated, in the weak form, using a third order dual operator splitting scheme (details within [9]). The integration scheme is coupled with a spectral–element discretization and solved in primitive variable form (for a review of the technique see [10]). The implementation of the spectral–element technique has been previously validated within [19]. The 2D spectral–element technique was implemented on a meridional semi–plane and extruded azimuthally using a Fourier expansion based on [1] which was previously implemented in [18]. A grid resolution study was performed at the highest Reynolds number ($Re = 22$) and grid independent convergence was observed (data not shown).

Boundary Conditions

The inlet and outlet boundary velocity boundary conditions are the analytic solution of rectilinear channel flow. The boundary

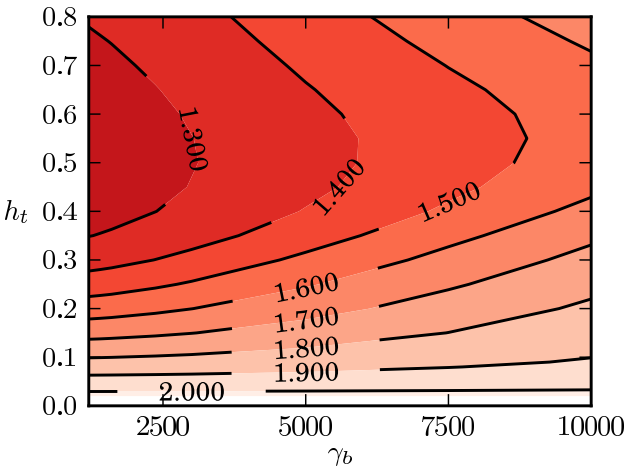

Figure 2: Normalized peak shear rate (χ) on thrombus surface plotted against h_t and γ_b. Darker red contours represent lower, and lighter contours higher values in shear rate.

conditions are expressed by:

$$u_x(y,z) = -\frac{1}{2\mu}\frac{\partial p}{\partial x}c^2\left[1-\left(\frac{z}{c}\right)^2 + 4\sum_{k=1}^{\infty}\frac{(-1)^k}{\alpha_k^3}\frac{\cosh\left(\frac{\alpha_k y}{c}\right)}{\cosh\left(\frac{\alpha_k b}{c}\right)}\times \cos\left(\frac{\alpha_k z}{c}\right)\right], \qquad \alpha_k = (2k-1)\frac{\pi}{2},$$

$$Q = -\frac{4}{3\mu}\frac{\partial p}{\partial x}bc^3\left[1-\frac{6c}{b}\sum_{k=1}^{\infty}\frac{\tanh\left(\frac{\alpha_k b}{c}\right)}{\alpha_k^5}\right].$$

The equations above from [14] where flow is in the x_+ direction. Domain extent ranges from $-b \le y \le b$ and $-c \le z \le c$. On the channel walls and the thrombus analogue surface, a no slip condition is imposed for velocity in addition to a Neumann boundary condition for pressure.

Particle Tracking Analysis

In addition to solving the momentum and continuity equations within an Eulerian framework, Lagrangian particles are introduced as platelet analogues. As the platelets are small with respect to the flow features it is presumed that the platelets are accurately modeled by infinitesimal massless particles. The particle tracking is implemented using the technique of [5] to preserve the accuracy of the spectral–element discretization. Particles are integrated forward in time using a 4th order Runge–Kutta technique. Given the steady state flow conditions within the domain, the Lagrangian behavior may be mapped onto the Eulerian grid. In particular, the temporal derivative of χ within the Lagrangian framework. To implement this the flow is seeded throughout the domain with particles. These particles are evolved for a short amount of time such that the temporal derivative may be calculated with a second order accurate finite difference scheme. The temporal derivative is then interpolated back onto the Eulerian grid using a radial basis function interpolation technique within overlapping sub–domains.

Results and Analysis

Peak Shear Rate

For each of the simulations performed the flow is time–stepped until a steady state is achieved. Subsequent to this the peak

shear rate is extracted for each case by computing the maximum across the nodal evaluation points, no interpolation was used. This is displayed as a contour plot in figure 2. For a given bulk shear rate, the peak shear rate is at a maximum at the minimum thrombus height. From this point a steady decrease in maximum shear rate is observed as the thrombus size increases to $h_t \simeq 0.5$. This decrease in shear rate maximum is attributed to the decrease in curvature as the thrombus increases in size. The curvature decrease is the result of the thrombus maintaining geometric similarity (that $\frac{h_t}{r} = 0.25$). As the thrombus size increases past $h_t \simeq 0.5$ a gradual increase in the shear rate maximum is observed. This increase in shear rate maximum is attributed to the occlusion of the channel as the thrombus grows (up to 15% of cross–sectional area). Similar behavior is observed over the full range of bulk shear rates. However, we do note that a trend of increasing non–dimensionalized shear rate (χ) is observed as shear rate increases. This increase is non–linear. This non–linear increase occurs concurrently with an ever–increasing forward–backward asymmetry as described within [3]. This non–linear effect is more pronounced at larger thrombus sizes. A Reynolds number based on thrombus sizes (Re_T) is defined as

$$Re_T = \frac{H_T \bar{U}}{\nu}. \tag{9}$$

This results in the range: $0.05 \leq Re_T \leq 22$. The variation occurs linearly with respect to both γ_b and H_T. The flow at the lowest Reynolds number ($Re_T = 0.05$) is nearly Stokesian (forward–backward symmetry). As Re_T increases, the non–linear affect of advection becomes stronger. This noticeably affects the shear rate maximum at $Re_T = O(1)$.

The variations in peak shear rate observed are relatively simple from a fluid dynamics point of view it does, however, have wider implications for the biology of the system. Previous studies (e.g. [12]) have completely neglected localized variations in shear rate. Under this paradigm, the Poiseuille flow model performs acceptably. Given that thrombus growth has been attributed to shear rate 'micro gradients' [13] this simplistic view of shear rate is no longer sufficient. The localized variations of shear rate are dependent on *Re* therefore future studies considering thrombus development must take care to characterize the results in terms of γ_b, *Re*, and the geometry of the system.

Shear Rate Gradients

The shear rate gradient,

$$\frac{D\chi}{Dt}, \tag{10}$$

was calculated using the previously described method. For each domain in which the Navier–Stokes equations were solved for, so to was the Lagrangian shear rate gradient. The resulting gradients are visualized as iso–surfaces surrounding the thrombus analogue. The structure of these gradients are not observed to significantly change with respect to γ_b. However the structure of the gradients does change with increasing h_t. Figure 3 shows iso–surfaces surrounding the maximum, and minimum, of shear rate gradient. Immediately it is noted that the maxima, unlike shear magnitude, or gradient with respect to spatial displacement, is located within the flow domain, rather than at the surface. As platelets are small with respect to the flow feature size, logically they may only experience temporal gradients. Therefore we expect shear rate gradient based behaviour to correspond to regions of temporal gradients. This theory is supported by *in vitro* experiments where bulk temporal gradient increased thrombus adhesion [8]. However there is insufficient *in vitro* evidence to further support this theory. Despite this, in all cases the regions of high shear rate gradient are located close to the thrombus surface. The region where platelets are consis-

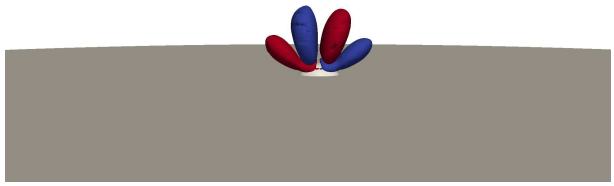

(a) $h_t = 0.08$

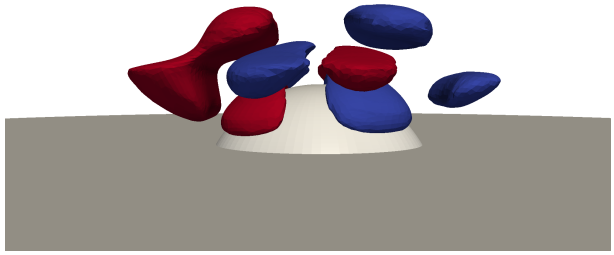

(b) $h_t = 0.35$

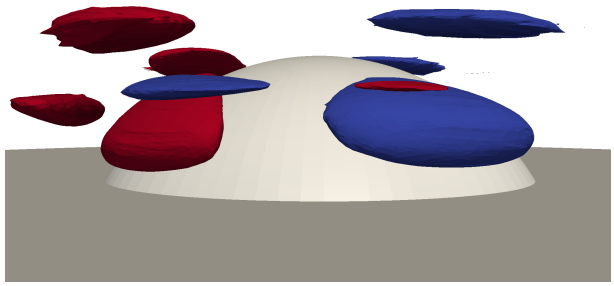

(c) $h_t = 0.8$

Figure 3: Iso–surfaces of shear rate gradient $\frac{D\chi}{Dt}$ at $\gamma_b = 3000$. In each of the cases the grey translucent surface represents the lower wall of the channel and the thrombus. The side and upper walls are not shown. The scale is fixed across each figure. In each case flow within the domain is left to right across the page. The positive (red) and negative (blue) iso–surfaces are set at the same amplitude, approximately one half of the positive gradient maxima.

tently flowing close to the thrombus and where platelets have the highest density due to the process of platelet marginalization by red blood cells [7]. The gradients observed are located such that they support the theory of platelet adhesion triggered by shear rate temporal gradients. Furthermore, it is noted that lobes of maximum shear extend into the domain suggesting that increased platelet bonding may occur throughout the flow, not localizied in the region near the thrombus surface. This behavior is seen under both *in vitro* and *in vivo* environments by Nesbitt et al [13].

A multi–lobed structure for shear rate gradient maxima and minima is observed within the domain. This structure is observed to gain complexity as the thrombus increases in size with respect to the channel. A 'chequerboard' pattern of positive and negative gradients is observed with respect to the flow direction. This implies that there may be multiple regions surrounding the thrombus where shear gradient triggered platelet adhesion is likely.

Conclusions

This numerical investiagation has explored the dynamics of shear rate, both in an Eulerian and Lagrangian sense, surrounding a thrombus analogue within an *in vitro* environment. The normalized shear rate (χ) is observed to change non–linearly over the range of Reynolds numbers appropriate for *in vitro* experiments ($O(0.1) \leq Re \leq O(10)$). Additionally the maximum shear rate a thrombus experiences was observed to dramatically decrease with increasing thrombus size. This points to the potential for stability of a thrombus with respect to shear rate dependent growth similar to the stability that may be observed *in vitro* and *in vivo*. Shear gradient, believed to be a stimulus for thrombus growth through platelet adhesion and activation, was observed to have a complicated structure near the thrombus. This structure extends into the flow suggesting platelet adhesion may not be localized to near the thrombus surface. Further investigation of shear rate gradients is required, with more realistic thrombus shapes, to better understand the implications of shear rate gradients on *in vitro* and *in vivo* flows. Experimental investigations are suggested to quantify whether shear gradients or shear is the dominant flow based criterion affecting platelet function and thrombus growth.

Acknowledgements

The authors thank VLSCI for the computational time provided under grant VR0023. CJB thanks the Monash Engineering Faculty for the ERLA funding his study.

References

[1] Blackburn, H. and Sherwin, S., Formulation of a Galerkin spectral element–Fourier method for three-dimensional incompressible flows in cylindrical geometries, *Journal of Computational Physics*, **197**, 2004, 759–778.

[2] Born, G. and Cross, M., The aggregation of blood platelets, *The Journal of Physiology*, **168**, 1963, 178.

[3] Butler, C. J., Sheard, G. J. and Ryan, K., Modelling variations in shear rate around a geometrically similar thrombus in–vitro, in *Seventh International Conference on Computational Fluid Dynamics in the Minerals & Process Industries*, editors P. J. Witt and M. P. Schwarz, CSIRO Australia, Rydges Hotel, Melbourne, Australia, 2009.

[4] Caro, C., Vascular fluid dynamics and vascular biology and disease, *Mathematical Methods in the Applied Sciences*, **24**.

[5] Coppola, G., Sherwin, S. and Peiro, J., Nonlinear particle tracking for high-order elements, *Journal of Computational Physics*, **172**, 2001, 356–386.

[6] Eisenberg, P. and Ghigliotti, G., Platelet-dependent and procoagulant mechanisms in arterial thrombosis, *International journal of cardiology*, **68**, 1999, 3–10.

[7] Fung, Y., *Biomechanics: mechanical properties of living tissues*, Springer, 1993.

[8] Goncalves, I., Nesbitt, W. S., Yuan, Y. and Jackson, S. P., Importance of Temporal Flow Gradients and Integrin alphaIIbbeta3 Mechanotransduction for Shear Activation of Platelets, *J. Biol. Chem.*, **280**, 2005, 15430–15437.

[9] Karniadakis, G., Orszag, S. and Israeli, M., High-order splitting methods for the incompressible Navier-Stokes equations, *Journal of Computational Physics (ISSN 0021-9991)*, **97**.

[10] Karniadakis, G. and Sherwin, S., *Spectral/hp Element Methods for Computational Fluid Dynamics*, Oxford University Press, 2005.

[11] Ku, D., Blood flow in arteries, *Annual Review of Fluid Mechanics*, **29**, 1997, 399–434.

[12] Kulkarni, S., Nesbitt, W., Dopheide, S., Hughan, S., Harper, I. and Jackson, S., Techniques to examine platelet adhesive interactions under flow, *Methods in Molecular Biology*, **272**, 2004, 165–186.

[13] Nesbitt, W., Westein, E., Tovar-Lopez, F., Tolouei, E., Mitchell, A., Fu, J., Carberry, J., Fouras, A. and Jackson, S., A shear gradient–dependent platelet aggregation mechanism drives thrombus formation, *Nature Medicine*, **15**, 2009, 665–673.

[14] Papanastasiou, T., Georgiou, G. and Alexandrou, A., *Viscous fluid flow*, CRC, 2000.

[15] Rodkiewicz, C., Sinha, P. and Kennedy, J., On the Application of a Constitutive Equation for Whole Human Blood, *Journal of Biomechanical Engineering*, **112**, 1990, 198.

[16] Savage, B., Almus-Jacobs, F. and Ruggeri, Z., Specific synergy of multiple substrate-receptor interactions in platelet thrombus formation under flow, *Cell(Cambridge)*, **94**, 1998, 657–666.

[17] Savage, B., Saldivar, E. and Ruggeri, Z., Initiation of Platelet Adhesion by Arrest onto Fibrinogen or Translocation on von Willebrand Factor, *Cell(Cambridge)*, **84**, 1996, 289–297.

[18] Sheard, G., Fitzgerald, J. and Ryan, K., Cylinders with square cross-section: wake instabilities with incidence angle variation, *Journal of Fluid Mechanics*, **630**.

[19] Sheard, G., Leweke, T., Thompson, M. and Hourigan, K., Flow around an impulsively arrested circular cylinder, *Physics of Fluids*, **19**, 2007, 083601.

[20] Wootton, D. and Ku, D., Fluid mechanics of vascular systems, diseases, and thrombosis, *Annual review of biomedical engineering*, **1**, 1999, 299–329.